Carburization Rates of Tungsten Powders

MEYER L. FREEDMAN
Refractory Metals Laboratory, General Electric Co., Cleveland 17, Ohio

PRODUCTION of the hardest grade of cemented tungsten carbide has classically required the use of a tungsten powder made by the reduction of $WO_3 \cdot H_2O$, precipitated tungstic acid (*5*). Tungsten powder made by reducing ammonium paratungstate has been considered less suitable for this purpose regardless of processing variations (*6*). Dawihl and co-workers used electron microscope and x-ray diffraction techniques to study tungsten and tungsten carbide powder intermediates (*9*). The paratungstate derived carbide was of lower hardness even though the metal and carbide powders were tested at the same crystallite sizes. The anomaly has not been explained, so that it is of interest to determine what properties of the tungsten powders may control the hardness of the carbide.

The reduction of tungsten oxide to metal and the carburization of the metal powder are generally carried out as topochemical processes, in which one solid phase is converted to another without the interposition of a gaseous or liquid state. The microcrystalline structure of the new phase should then depend in some degree on that of the starting material. In particular, the particle size and the extent of crystalline imperfections should depend on the initial solid phase (*21*). Tungsten powders are graded primarily by particle size, which is commonly measured by gas permeability methods (*1*). The particle-size distribution can be determined by turbidimetric sedimentation techniques although it is difficult to distinguish primary particles from aggregates (*13*). X-ray diffraction indicates the size of the crystalline subgrains of the metal particles, but requires an uncertain correction for lattice distortions (*11*).

The chemistry of tungsten carburization and the technology of cemented carbide production have been reviewed in detail (*3, 14, 16, 22, 23*). Tungsten powder is intimately mixed with carbon and heated to 1400° C. or higher. Pirani and Sandor carburized 0.2 mm. tungsten beads and obtained coatings of carbide separated from the metal by sharp diffusion boundaries (*18*). Preferential penetration along grain boundaries was not observed, and the rate determining step was diffusion of carbon through the tungsten carbide layer, so the reaction was not apparently structure sensitive.

The differences in product quality obtained with different tungsten powders of the same particle size can be explained only if the carburization of tungsten powder is a structure sensitive reaction. The crystallite size of the tungsten carbide will depend on the relative rates of nucleation and formation of this phase. Grain and subgrain boundaries of the tungsten particle may serve as nucleation sites as well as provide paths for rapid diffusion. The internal structure of the tungsten powders as possibly modified by milling and annealing should determine the carburization rate at a given particle size.

This hypothesis was tested by measuring the carburization rates of tungsten powders produced both from precipitated tungstic acid and from ammonium paratungstate crystals. The latter compound is usually reduced to metal in two stages, with the intermediate formation of either yellow oxide or of partially reduced blue or brown oxides. A great variety of tungsten powders can apparently be produced from any of these oxides by variations in reduction conditions. The tungsten powders used were obtained from various commercial sources and were selected on the basis of similar particle size.

EXPERIMENTAL

An adaptation of differential thermal analysis techniques was used. Since the carburization reaction is exothermic, the temperature of a rapidly heated mixture of tungsten and carbon will rise faster than the temperature of an inert reference material under the same conditions. The voltage generated by a thermocouple placed in the reaction mixture was opposed by that of a thermocouple in the reference material and the differential voltage was recorded as a function of time. The relative carburization rate was measured in millivolts as the peak of this differential voltage-time curve. A rapid heating rate was used to cover the 800° to 1400° C. temperature range over which the reaction takes place in order to minimize annealing of the metal powder during the reaction.

Apparatus. The carburization cell was designed to fit an existing horizontal tube furnace. An iron tube 2 feet long extended from an alumina furnace tube, 2 feet long by 2 inches I.D., which carried a stream of hydrogen gas. The current through the molybdenum heating element was controlled manually by a variable reactance transformer and temperature measurements were made with an optical pyrometer.

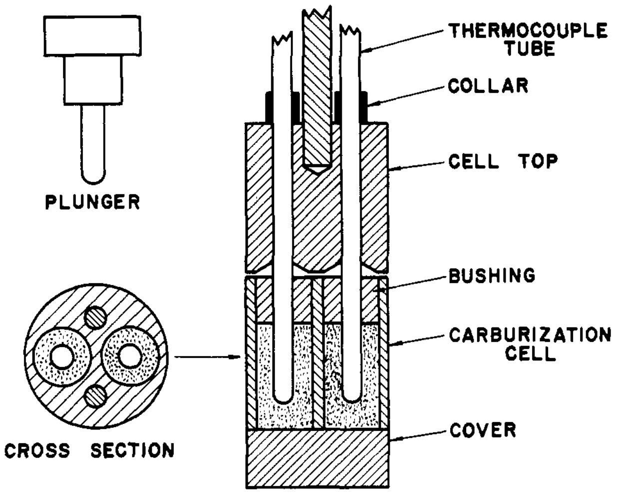

Figure 1. Carburization cell

The cell was constructed by drilling a ⅞-inch diameter carbon bar as shown in Figure 1 and then sawing it in two. A carbon baffle was permanently attached to the top half of the cell by a carbon rod 8 inches long and ⅜ inch in diameter. The parts of the cell were held together by ¼-inch-diameter carbon dowels. After initial assembly the cell and baffle were sanded to slide freely through the furnace tube. All parts were marked to assure exact reassembly and the right side of the cell and thermocouple were always used for the reference material. Platinum-platinum 13% rhodium thermocouples of 20-mil wire 37½ inches long were used. The thermocouple protection tubes were of mullite, 12 inches long by 7 mm. in O.D. Porcelain collars were cemented into place 3½ inches from the closed ends, and the open ends were sealed to extension tubes of 10-mm. borosilicate glass 2 feet long. Double-hole porcelain insulators 5 mm. O.D. by 36 inches long were used. The differential voltage was recorded on a Brown

Dynamaster having a full scale range of 10 mv. at a chart speed of 5 minutes per inch.

Procedure. The tungsten powder samples were mixed with 10% by weight of carbon black, milled for 6 hours using tungsten rods as the grinding media, and tested under conditions of equal mass and density. The open carburization cell was fastened to the cover and 35.00 grams of the powder mixture was compressed to 10-ml. volume into the left cavity by the steel plunger using hand pressure. The right cavity was similarly filled using the standard reference mixture of tungsten carbide and 4% by weight of carbon black. The carbon bushings were then inserted on top of the charges, the cell top was fastened in place, and the *thermocouple tubes were inserted.* Figure 2 shows the assembled cell.

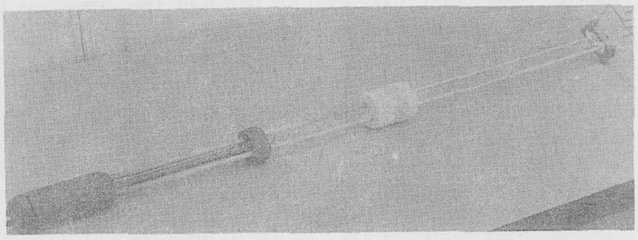

Figure 2. Assembled carburization cell

The filled cell was inserted into the furnace-tube extension and positioned for 15 minutes at the cold end, where air and moisture could be eliminated at 300° C. in the stream of hydrogen. Sliding the cell further into the furnace then gave a range of annealing temperatures. A Brown potentiometer was used to measure the annealing temperature, and the borosilicate tubes were marked so that the position of the cell in the furnace tube could be readily duplicated. The cell was then pushed to the center of the heated zone and the differential curve was recorded. Figure 3 shows a typical differential curve and heating curves for both the sample and the reference material. The time required to reach the peak differential voltage was of the order of 5 minutes for a 300° C. anneal and only 2 minutes when the cell was heated to 750° C. before insertion into the high temperature zone. *After 2 or 3 minutes more, when* the differential voltage had dropped to a low value, the cell was withdrawn into the low temperature zone for cooling before removal from the furnace.

Triplicate determinations made with a furnace wall temperature range of 1410° to 1425° C. and 45 minute annealing at 750° C. gave values of 3.13, 3.15, and 3.15 mv. for a standard deviation of only 0.01 mv. However, the temperature could not be controlled so closely over long periods. Actual furnace temperature varied from 1405° to 1440° C. and the annealing temperatures varied over a 50° range. Duplicate determinations were made for each sample and the average values taken. The maximum difference observed in duplicate runs on 8 samples was 0.07 mv. with an average of 0.03 mv. It was considered that there was significant difference between samples when the average of duplicate determinations differed by 0.10 mv. or more.

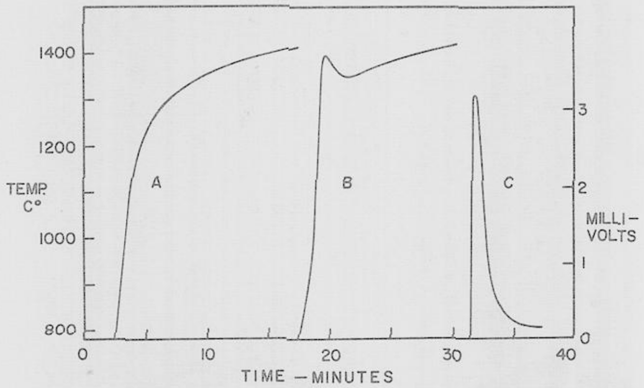

Figure 3. Typical heating rate curves

A. Reference
B. Sample
C. Differential

Results. Table I characterizes four tungsten powders of fine grain size and high purity. Powder 1 was known to have produced tungsten carbide cemented with 3% of cobalt having a high hardness of 92.0 Rockwell A. Powders 2 and 2a were very similar to powder 1 in physical characteristics, but were not considered as suitable for making this grade of tungsten carbide.

Powder 1 carburized more rapidly than powder 2, but this order was reversed by annealing, as shown in Table II. The carburization cell was held for 45 minutes at temperatures shown in the table before being moved into the *1400° C. zone. The carburization products were examined* by x-ray diffraction. Powder 1 was completely converted to WC by the few minutes of heating at 1400° C., without pre-annealing. Under the same conditions, the x-ray diffraction pattern of the carburized powder 2 showed the presence of W_2C and W as well as WC. However, after annealing at 750° C., powder 2 was also completely converted to WC by the test carburization. X-ray diffraction examination of tungsten-carbon black mixtures after 45 minutes of annealing at 750° C. showed both WC and W_2C to be absent, for powders 1 and 2, in agreement with reports that the carburization rate of tungsten is very slow below 800° C. (*22*).

Table I. Tungsten Powder Characteristics

	Powder Number			
	1	2	2a	3
		Paratungstate		
Source	Precipitated $WO_3 \cdot H_2O$	Brown oxide	Brown oxide	Blue oxide
Fisher size, μ	1.35	1.33	1.27	1.18
Particle size, %[a]				
1μ	28.5	32.2	29.6	54.8
2μ	51.2	45.2	55.0	43.0
3μ	12.3	12.6	11.1	2.1
Mean Particle diam., μ	1.43	1.40	1.36	0.91
Analysis, %[b]				
Na	0.002	0.001	0.005	0.002
K	0.003	0.005	0.008	0.005
Mo	0.004	0.001	...	0.004
Fe	0.011	0.002	0.005	...

[a] Weight per cent by turbidimetric sedimentation.
[b] Spectrographic; impurities above 0.001%.

Table II. Effect of Annealing Temperature on Carburization Rate

Temp., ° C.	Powder 1, mv.	Powder 2, mv.
25	...	2.31
300	2.69	2.30
500	2.65	2.32
750	2.85	3.41
890	...	2.87

The relative carburization rates of a series of tungsten powders are listed in Table III. Powders 1a and 2a were different lots of the same types as 1 and 2, respectively. None of the other samples carburized at a high rate despite the heat treatment.

The effects of the heat treatment on the microcrystalline *structures of the tungsten powders were investigated by*

Table III. Carburization Rates of Tungsten Powders

(Pre-annealed at 750° C.)

Powder No.	Source	Subsieve Size, μ	Carburization Rate, mv.
1	$WO_3 \cdot H_2O$	1.35	2.85
1a	$WO_3 \cdot H_2O$	1.34	2.91
2	Brown oxide	1.33	3.41
2a	Brown oxide	1.27	3.14
3	Blue oxide	1.18	2.45
4	Yellow oxide	1.17	2.43
5	Blue oxide	1.39	2.17
6	Brown oxide	1.24	2.53

x-ray diffraction. The width of the 411 line was measured at half its peak intensity, using an x-ray diffractometer with copper K beta radiation. Correction was made for instrumental line broadening, but was not attempted for the component of line broadening due to lattice distortions. A mean crystallite size was then calculated from the relation (*11*)

$$D_{hkl} = \frac{0.9\lambda}{\beta_{1/2} \cos \theta}$$

The calculated values are shown in Table IV.

Table IV. Mean Crystallite Size from Line Broadening

Powder	1	2	2a	3
As received, μ	0.06	0.18	0.25	0.06
Milled, μ	0.04	0.13	0.17	0.05
Annealed at 750° C. μ	0.05	0.09	0.12	0.04

The apparent reduction in crystallite size effected by milling is considered due to increased lattice distortion. Annealing partially eliminates this distortion, so that the original size should be regained, at least in part. Powder 1 shows this action. On the other hand, annealing greatly reduces the crystallite size of powders 2 and 2a, even though the degree of lattice distortion must have been reduced. This is evidence for polygonization, the alignment of dislocations to produce new subgrain boundaries (*8*). This effect was very small with powder 3.

The role of grain boundaries in the carburization of tungsten was investigated on a macro scale by the use of tungsten bicrystals. Rods of high purity tungsten, 0.25 cm. in diameter, were zone refined by electron bombardment to produce tungsten single crystals (*4*). Some specimens formed with two crystals occupying the full cross section of the rod and were used in this work. A short section of the bicrystal was deformed by bending slightly and then placed in a graphite boat with a covering of carbon black. This was given the standard heat treatment, 45 minutes at 750° C., and then pushed into the 1400° C. furnace zone for 5 minutes. The surface of the carburized rod became blue. Under the microscope discontinuous patches of carbide were seen to center at etch pits. The rod was ground away to a depth of 0.1 cm. and examined metallographically. Figure 4 shows a section in the interior of the rod. The grain boundary is nearly filled by carbide precipitate, while adjoining subgrain boundaries are clear. Figure 5 shows a section at the surface of the rod. Here carbide precipitates are visible within the subgrain boundaries and within the subgrains as well.

The carburization rate measurements had been made with a standard excess of carbon black in order to avoid possible variations in mixing. Stoichiometric tungsten carbide is required for hardness testing. Accordingly, the proportion of carbon black was reduced to 6.25% for a sample of powder 2a and the carburization was carried out at 1400° C., after 45 minutes of annealing at 750° C. The product was a soft grey powder which contained 6.09% of carbon. This was milled with 3% of cobalt powder, pressed into a ¼-inch pellet, and sintered in a hydrogen furnace for 1 hour at 1425° C. The Rockwell A hardness of the pellet was 92.4, although the microstructure indicated some unrecrystallized tungsten carbide to be present.

DISCUSSION

The effect of microcrystalline structure on carburization kinetics are shown by the experiments with tungsten bicrystals. Carbon diffuses rapidly through the tungsten at the 1400° C. reaction temperature and tungsten carbide precipitates in areas where the atomic rearrangement from the cubic tungsten lattice to hexagonal tungsten carbide is easiest: grain boundaries, surface pits, and lattice defects within the grain. Identical phenomena have been noted for the carburization of some ferrous alloys (*19*). The large specific surface areas of the fine tungsten powders apparently permit carbon to dissolve in metal more rapidly than the tungsten carbide phase can crystallize from the metal, at the test temperature. In fact, the tungsten powders of smaller particle size and hence of largest specific surface carburized more slowly than the coarser powder.

The tungsten powders made from $WO_3 \cdot H_2O$ (1 and 1a) have an optimum grain size and small crystallite size for rapid carburization. The internal grain boundary surface area is large. Powder 3 has a similar crystallite size, but smaller grain size so the internal surface area is smaller.

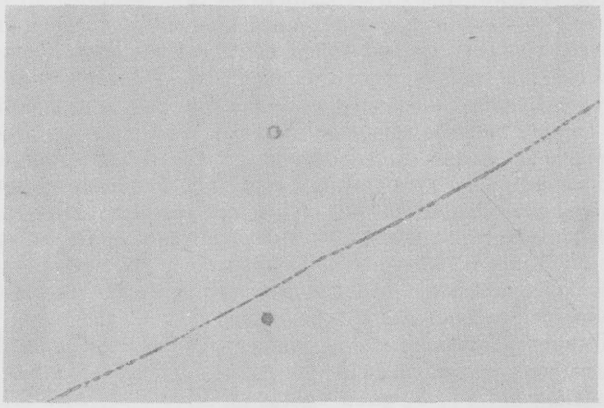

Figure 4. Carbide precipitate in grain boundary

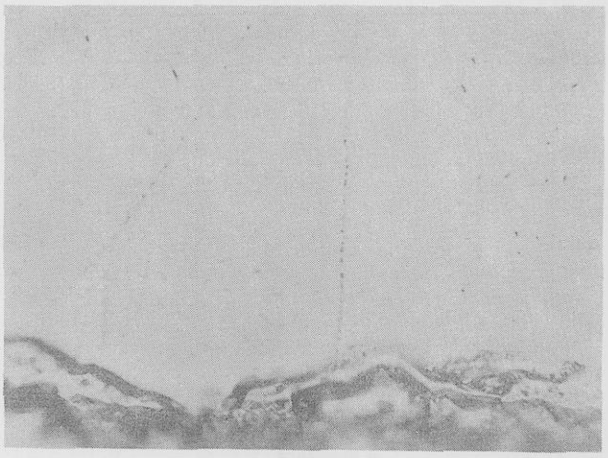

Figure 5. Carbide precipitate near surface

Powders 2 and 2a have grain sizes similar to that of powder 1 but the crystallite size is large. After annealing it is still larger than that of powder 1, but the carburization rate is now more rapid than powder 1. The new subgrain boundaries formed by polygonization are apparently more reactive for tungsten carbide crystallization than pre-existing internal surfaces.

The temperature dependence of the microstructure of cold worked tungsten has been reviewed by Pugh *(20)*. Polygonization, the alignment of dislocations into subgrain boundaries, is considered to be the major structural change which takes place on annealing cold worked tungsten for periods of the order of an hour at 700° to 800° C. At higher temperature subgrain growth takes place with a coarsening of the microstructure and a reduction of grain boundary area. The subgrain boundaries formed by polygonization may have a different structure than other grain boundaries, as has been demonstrated by the electron microscope investigation of Jones *(10)*. Polygonized boundaries in tungsten foils appeared as parallel rows or hexagonal nets of dislocations closely spaced at 0.01 to 0.04 micron.

Only powders 2 and 2a had sufficiently large crystallites to clearly exhibit polygonization. Size effects are common in the working and annealing of tungsten wires. *(24)*. Opinsky has studied the microstructure of tungsten wires and found that the crystallite size could not be reduced below 0.03 microns by cold deformation *(15)*. The size of polygonized subgrains depends also on the amount of cold work absorbed. Thus, for slightly bent molybdenum crystals polygonization produced subgrains 3 to 4 microns in diameter *(2)*. The subgrains produced in powder 2 were of the order of 0.1 micron. Powders 1 and 3 already had mean crystallite sizes of the order of 0.06 micron, so that the formation of 0.1 micron subgrains by polygonization was impossible. Dislocations presumably migrated to existing boundaries in these cases.

Powders 1 and 3 were apparently not plastically deformed by milling because of their small crystallite sizes. Petch has related the minimum shear stress for plastic flow to grain size *(17)*. However, Koo found that the lower yield stress for tungsten wires was a function of crystallite size rather than grain size *(12)*. The application of a shear stress greater than the critical value moves dislocations along their glide planes resulting in plastic deformation. Interaction of the moving dislocations produces new dislocations in great number by regenerative multiplication mechanisms *(7)*. Polygonization aligns some of these dislocations into new subgrain boundaries while their total number is greatly reduced, since positive and negative dislocations cancel each other. The carburization rate would be decreased by polygonization if diffusion of carbon through the metal was rate controlling. Dislocations provide routes for rapid diffusion. The observed rates show that the carburization of fine tungsten powders at 1400° C. is a structure-sensitive reaction which is not diffusion controlled.

The results of Pirani and Sandor are different from those of this investigation because of the great difference in materials. The prior investigators carburized arc melted tungsten beads of very low specific surface and large crystal size. Once the surface was covered with tungsten carbide, presumably after the few grain boundaries were saturated, diffusion through the surface layer was rate controlling. The crystal habit of the tungsten carbide will also depend on its crystallization site. Surface reaction produces columnar grains while the carbide formed at grain boundaries has a laminar structure.

The reputed high hardness of cemented tungsten carbide produced from powder 1 is presumably due to the small crystallite size of the carbide resulting from the rapidity of the carburization reaction. Such tungsten carbide would be expected to react rapidly with liquid cobalt during the cementing operation. Introduction of the annealing step makes possible the production of similar carbide from powder 2. Dawihl noted that tungsten powder made from $WO_3 \cdot H_2O$ carburized completely in 15 minutes at 1400° C., while 30 minutes were required for tungsten powder made from the paratungstate, but he did not investigate the effects of heat treatment on the carburization rates.

ACKNOWLEDGMENT

The author thanks W.A. Buerkel for supplying the tungsten powders and the particle size data. Thanks are also due to Sam Leber and U.E. Wolff for x-ray and metallography.

LITERATURE CITED

(1) Am. Soc. Testing Materials, "Average Particle Size of Refractory Metals and Compounds by Fisher Sub-Sieve Sizer," ASTM B 330-58T.
(2) Aust, K.T., Maddin, R., *Acta Met.* **4**, 632 (1956).
(3) Burden, H., Barker, A., *J. Inst. Metals* **75**, 51 (1948).
(4) Carlson, R.G., *J. Electrochem. Soc.* **106**, 49 (1959).
(5) Dawihl, W., "A Handbook of Hard Metals," p. 47, Philosophical Library, New York, 1955.
(6) Dept. of Commerce, Office of Tech. Serv. "The German Hard Metal Industry," **PB 81624**, 1945.
(7) Frank, F.C., "Chemistry of the Solid State," Chap. I, Garner, W.E., ed., Academic Press, New York, 1955.
(8) Gilman, J.J., *Acta Met.* **3**, 277 (1955).
(9) Hendus, H., Dawihl, W., Bartsch, G., *Z. Metallk.* **48**, 615 (1957).
(10) Jones, F.O., *J. Less-Common Metals* **2**, 163 (1960).
(11) Klug, H.P., Alexander, L.E., "X-Ray Diffraction Procedures," p. 512, Wiley, New York, 1954.
(12) Koo, R.C., *J. Less-Common Metals* **3**, 412 (1961).
(13) Michaels, A.I., in "Symposium on Particle Size Measurements," p. 207, ASTM Special Techn. Publ. No. **234**, 1959.
(14) Mitchell, A.D., Rees, R.W., *Ind. Eng. Chem.* **52**, 94 (1960).
(15) Opinsky, A.J., *J. Appl. Phys.* **33**, 708 (1962).
(16) Orton, G.W., "Phase Equilibrium of Tungsten-Carbon Systems," Ph. D. thesis, Dept. of Met. Eng., Ohio State University, 1961.
(17) Petch, N.J., *J. Iron Steel Inst. (London)* **173**, 25 (1953).
(18) Pirani, M., Sandor, J., *J. Inst. Metals* **73**, 385 (1947).
(19) Pomey, G., Trans. AIME **218**, 310 (1960).
(20) Pugh, J., Paper 1X, "Plansee Proceedings 1958," Benesovsky, E., ed., Metallwerk Plansee A.G., Reutte/Tyrol (1959).
(21) Remy, H., "Treatise on Inorganic Chemistry," Vol. **2**, p. 756, Elsevier, New York 1956.
(22) Schwarzkopf, P., Kieffer, R., "Refractory Hard Metals," Macmillan, New York 1953.
(23) Schwarzkipf, P., Kieffer, P., "Cemented Carbides," Macmillan, New York 1960.
(24) Smithels, C.J., "Tungsten," p. 157, Chem. Publ. Co., New York 1953.

Received for review December 11, 1961. Accepted July 5, 1962. Division of Industrial and Engineering Chemistry, 141st Meeting, ACS, Washington, D. C., March 1962.